17. Averill, F. W. & Painter, G. S. Symmetrized partial-wave method for density functional cluster calculations. *Phys. Rev. B* **50,** 7262–7267 (1994).
18. Painter, G. S., Becher, P. F., Shelton, W. A., Satet, R. L. & Hoffmann, M. J. Differential binding energies: effects of rare-earth additions on grain growth of β-Si_3N_4 and ceramic microstructure. *Phys. Rev. Lett.* submitted.

Acknowledgements We thank R. L. Satet and M. J. Hoffmann for supplying the silicon nitride ceramics used in this study. This work was supported by the US Department of Energy, Office of Basic Energy Sciences, Division of Materials Sciences and Engineering under contract with UT-Battelle, LLC. N.S. is a fellow of the Japan Society for the Promotion of Science (JSPS).

Competing interests statement The authors declare competing financial interests: details accompany the paper on **www.nature.com/nature**.

Correspondence and requests for materials should be addressed to N.S. (shibatan@ornl.gov).

Predictability of El Niño over the past 148 years

Dake Chen[1,2], Mark A. Cane[1], Alexey Kaplan[1], Stephen E. Zebiak[1] & Daji Huang[2]

[1]*Lamont-Doherty Earth Observatory of Columbia University, Palisades, New York 10964, USA*
[2]*Laboratory of Ocean Dynamic Processes and Satellite Oceanography, State Oceanic Administration, Hangzhou, China*

Forecasts of El Niño climate events are routinely provided and distributed, but the limits of El Niño predictability are still the subject of debate. Some recent studies suggest that the predictability is largely limited by the effects of high-frequency atmospheric 'noise'[1–7], whereas others emphasize limitations arising from the growth of initial errors in model simulations[8–10]. Here we present retrospective forecasts of the interannual climate fluctuations in the tropical Pacific Ocean for the period 1857 to 2003, using a coupled ocean–atmosphere model. The model successfully predicts all prominent El Niño events within this period at lead times of up to two years. Our analysis suggests that the evolution of El Niño is controlled to a larger degree by self-sustaining internal dynamics than by stochastic forcing. Model-based prediction of El Niño therefore depends more on the initial conditions than on unpredictable atmospheric noise. We conclude that throughout the past century, El Niño has been more predictable than previously envisaged.

Present estimates of El Niño's predictability are mostly based on retrospective predictions for the last two or three decades, encompassing a relatively small number of events[8–11]. With so few degrees of freedom, the statistical significance of such estimates is questionable. In principle, predictability can also be estimated by perturbing initial conditions in numerical model experiments, but the answer is model dependent, and existing models have not been shown to be realistic enough for this purpose. El Niño is evident in instrumental observations dating back to the mid-nineteenth century and in proxy data sets over much longer periods, but no successful attempt to 'hindcast' the historic El Niño events before the mid-twentieth century has been reported. This is due partly to the lack of adequate data for model initialization and partly to the inability of present models to make effective use of available data. The study reported here represents the first (to our knowledge) retrospective forecast experiment spanning the past one-and-a-half centuries, using only reconstructed sea surface temperature (SST) data[12] for model initialization.

The intrinsic predictability of El Niño is surely limited, but there has been considerable debate about what the limitations really are[1,13,14]. Classic theories consider El Niño and the Southern Oscillation (ENSO) as a self-sustaining interannual fluctuation in the tropical Pacific[15,16], being chaotic yet deterministic[17,18]. Thus its predictability is largely limited by the growth of initial errors, and the potential forecast lead time is likely to be of the order of years[8,10,19]. On the other hand, some recent studies emphasize the importance of atmospheric noise[2–4], particularly the so-called westerly wind bursts in the western equatorial Pacific[5–7]. In such a scenario, ENSO is a damped oscillation sustained by stochastic forcing, and its predictability is more limited by noise than by initial errors. This implies that most El Niño events are essentially unpredictable at long lead times, because their development is often accompanied by high-frequency forcing. Such a view is not supported by the present findings.

The observed and predicted SST anomalies averaged in the central equatorial Pacific are shown in Fig. 1a. (See Methods section

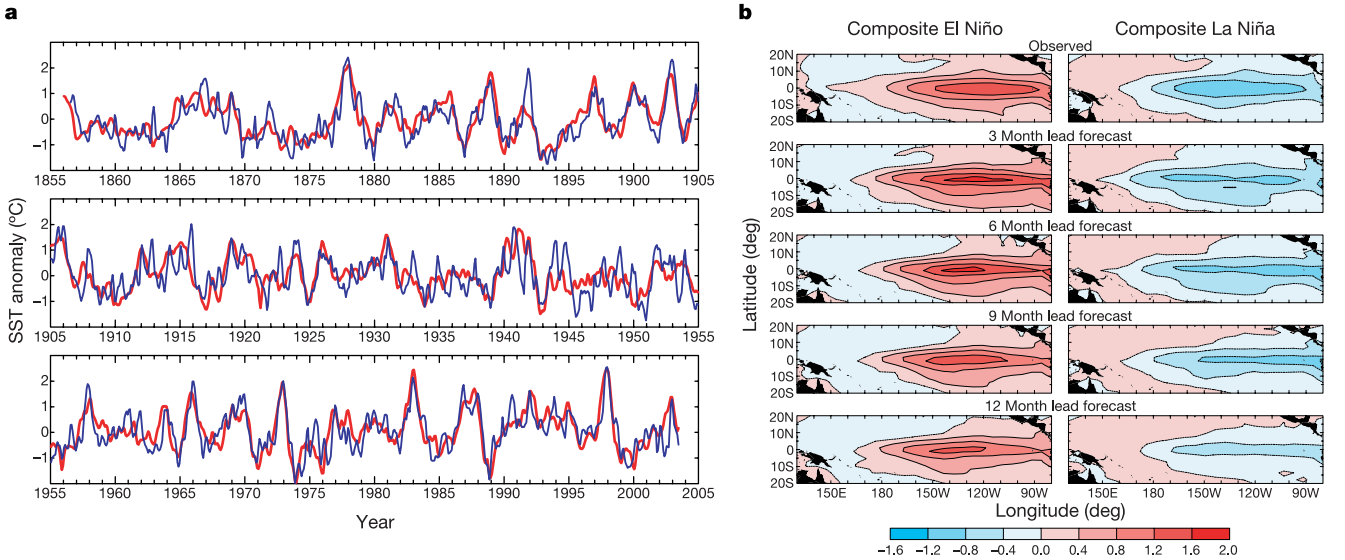

Figure 1 Retrospective predictions of El Niño and La Niña in the past 148 yr. **a,** Time series of SST anomalies averaged in the NINO3.4 region (5° S–5° N, 120–170° W). The red curve is monthly analysis of ref. 12 and the blue curve is the LDEO5 prediction at 6-month lead. **b,** Composite El Niño and La Niña from 24 warm events and 23 cold events. Top panels are observations, and the rest are predictions at different lead times. The colour bar shows the range of SST anomalies in degrees Celcius.

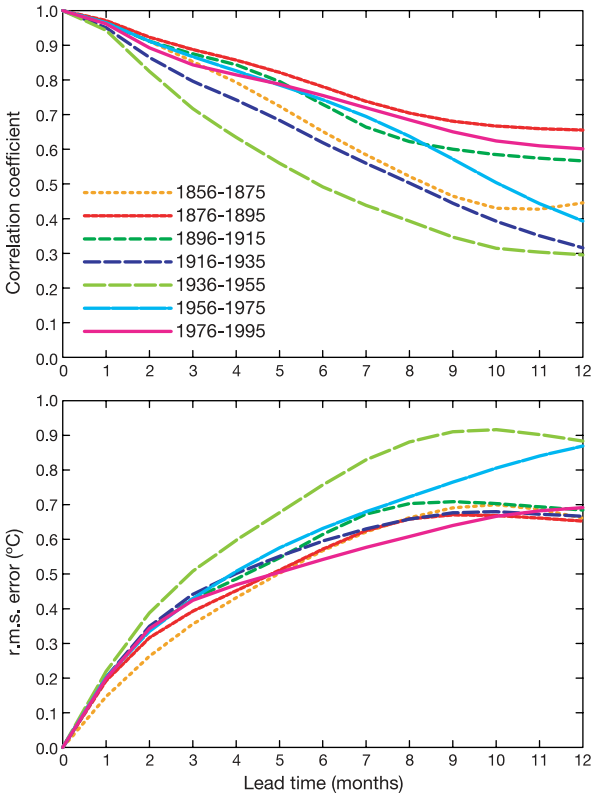

Figure 2 Anomaly correlations and r.m.s. errors between the observed and the predicted values of the NINO3.4 index. These are shown as a function of lead time, for seven consecutive 20-yr periods since 1856.

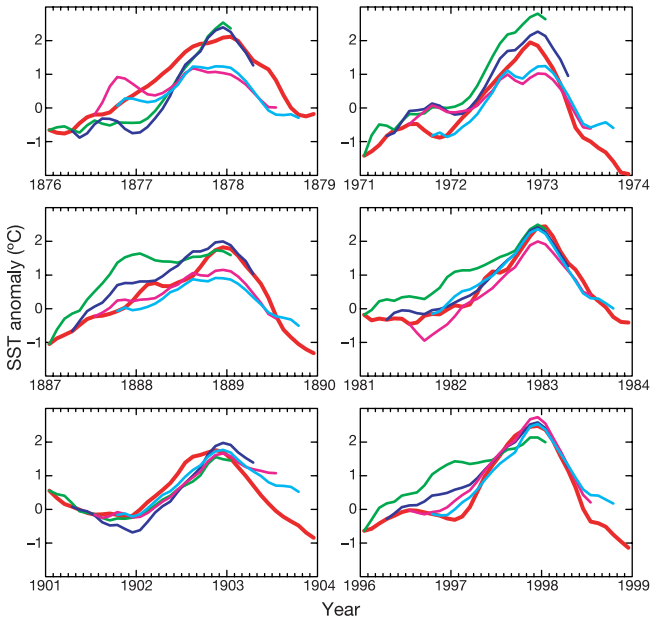

Figure 3 Six of the largest El Niños since 1856. The thick red curves are observed NINO3.4 SST anomalies, and the thin curves of green, blue, magenta and cyan are predictions started respectively 24, 21, 18 and 15 months before the peak of each El Niño.

for a description of the model and data used in this study.) At a 6 month lead, the model was able to predict most of the warm and cold events that occurred in the past 148 yr, especially the relatively large El Niños and La Niñas. The characteristics of the interannual variability obviously have changed with time. Although the strong and regular oscillations in the late twentieth century resemble what happened about a century earlier, there were relatively quiet periods without much activity. If we define an El Niño as a warm event when the NINO3.4 anomaly index is greater than 1 °C, and a La Niña as a cold event of the same amplitude, then there have been 24 of the former and 23 of the latter since 1856. Composites of these observed El Niños and La Niñas are displayed in Fig. 1b, together with corresponding forecast composites. On average, the spatial patterns of both El Niño and La Niña are well captured by the model.

ENSO's predictability depends on the time period from which it is estimated[9,20,21]. This is evident in Fig. 2. For the seven sub-periods of 20 yr each, both anomaly correlations and r.m.s. errors vary over significant ranges, especially at longer lead times. The periods with the highest overall scores, 1876–95 and 1976–95, are dominated by strong and regular ENSO events. Whereas the high scores for the 1976–95 period may not be surprising because the model was trained using data from part of this period, the even higher scores for the 1876–95 period, which is free of artificial skill, indicate that the large El Niños and La Niñas are highly predictable, even with a simple model initialized with only SST data. The lower skill in other periods is a result of there being fewer and smaller events to predict. For instance, during the 1936–55 period, when the predictability was the lowest by both measures, there were no El Niños except for a prolonged warm event in 1940–42.

Figure 3 shows long-lead forecasts for six of the largest warm episodes (as measured by peak NINO3.4 SST) in the past 148 yr. In all cases, the model was able to predict the observed strong El Niños two years in advance, though some errors exist in the forecasted onset and magnitude of these events. The implication is that the evolution of major ENSO events is largely determined by oceanic initial conditions, and that the effect of subsequent atmospheric noise is generally secondary. It is interesting to note that the model predicts the strong El Niño events in the late nineteenth century, which are notorious for their global impact. These events have been implicated[22] in the deaths of tens of millions of people in India, China, Ethiopia, Northeast Brazil and elsewhere. (The disastrous failure of the Indian monsoon in 1877 prompted the establishment of the Observatory in India, later the venue for the work of Walker that forms the foundation of modern understanding of ENSO.) The predictions shown here are, to our knowledge, the first successful retrospective forecasts of these significant historic events.

It has long been recognized that there is a so-called spring barrier in ENSO prediction, a drop of skill in persistence and in all model forecasts across the boreal spring. The skill of our model is also somewhat season-dependent (Fig. 4), as indicated by the relatively low correlations at spring verification time (the straight lines in the figure), but this spring barrier in model prediction is not as severe as that in persistence or in most other forecast models[23]. When the model predictions are verified against the observed anomalies exceeding ± 0.7 °C, the skill is much higher and the model can predict across two spring barriers for most start months. It seems that the model does well as long as there is a substantial signal to predict, which is consistent with the results of Figs 2 and 3. There are also some indications of an 'autumn barrier' for lead times longer than one year. This is probably due to the seasonal dependence of the discharge/recharge cycle of the equatorial heat content (or sea level), which leads the SST anomaly by 6–8 months and plays a crucial role in ENSO[24,25,26].

In summary, we have performed a retrospective ENSO forecast experiment for the past one-and-a-half centuries, which is several times longer than any previous experiments of this kind. Although the model was trained with recent data, it showed high skill in predicting the historic El Niño events back to the nineteenth century. Most importantly, we demonstrated that the large El Niños are predictable at long lead times. As our model has a self-sustaining internal oscillation and it does not invoke any stochastic

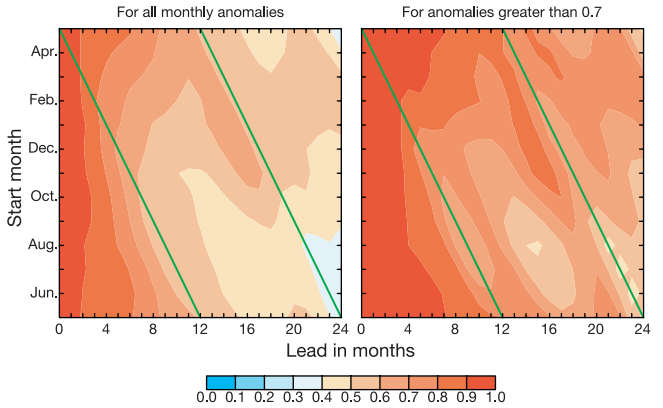

Figure 4 Correlations between observed and predicted NINO3.4 SST anomalies for the 1856–2003 period. These are shown as a function of start month and lead. The straight green lines denote the verification month of May. The left panel is based on all monthly anomalies, while the right panel is for anomalies with amplitudes greater than 0.7 °C. The colour bar shows the range of correlation coefficients.

forcing, this suggests that predictions depend more on initial conditions that determine the phase of ENSO, than on unpredictable atmospheric noise. Although westerly wind bursts do affect the exact onset time and perhaps the amplitude of El Niño, the gross features of ENSO seem to be coded in the large-scale dynamic state. Our results favour the interpretation that the enhanced wind burst activity in the boreal spring preceding large El Niño events is a consequence of those ongoing events[27] rather than a cause[1]. A practical consequence of our results is a more optimistic view of the possibility of skilful long-lead forecasts of El Niño.

One might suspect that this model does so well in predicting big El Niños because it always wants to predict such events, which means that it might produce as many false alarms as good predictions. To address this issue, we calculated NINO3.4 anomaly correlations for all predicted anomalies exceeding $\pm 0.7\,^{\circ}\mathrm{C}$ in the 1856–2003 period, and they are 0.58, 0.58 and 0.53 at 18, 21 and 24 month lead times, respectively. These values are about 0.08 smaller than those calculated for observed anomalies exceeding $\pm 0.7\,^{\circ}\mathrm{C}$ (right panel of Fig. 4), still far above the 95% significance level. This is consistent with the notion that although the model does not work as well during relatively quiet periods, model predictions are not severely plagued by false alarms.

The success of our experiment validates the reliability of the SST data set used here[12]. (We obtained similar results with several other newly reconstructed SST data sets[28,29].) However, because SSTs are the only data used for model initialization, and because our model is highly simplified and far from perfect, the predictive skill demonstrated here is a lower bound on El Niño's predictability—there is surely room for improvement. As mentioned above, the model's most notable difficulty is in predicting small events and occasions when no events occurred. The key to overcoming this difficulty is to design a data assimilation procedure that can pick the subtle information most relevant to ENSO out of a noisy background. □

Methods

The model used in this study, called LDEO5, is the latest version of an intermediate ocean–atmosphere coupled model[15,16] widely applied to ENSO investigation and prediction. It differs from its predecessor LDEO4[30] in its improved ability to assimilate SST data, which is crucial here as only reconstructed SST data sets are available for such a long-term experiment. In LDEO5, an assimilated SST field not only directly affects the surface wind field as in LDEO4, but also has a persistent effect on the coupled system. The improvement was achieved by including a bias correction term in the model SST equation that statistically corrects for model deficiencies in parameterizing subsurface temperature and surface heat fluxes. The correction was estimated inversely by fitting model SST tendency to observation using data from 1980–2000, and a regression relating this term to the multivariate model state was obtained in the space of empirical orthogonal functions, using the method of ref. 30. Based on this regression, an interactive correction of SST was then implemented in the model.

The internal variability of LDEO5 is similar to that of LDEO4[30]; it generates a self-sustaining oscillation with periods of 3–5 yr and amplitudes close to those of observed El Niños. However, the new version has a higher predictive skill when multiple data sets—sea level, winds, SST—are used for initialization, and its skill decreases only slightly when assimilating only SST data. We have to rely on SST data here because tropical Pacific sea level observations are virtually non-existent before 1970, and historic wind information is sparse and poorly calibrated. Note that in the coupled initialization procedure of the LDEO forecast system, assimilated SST data are not simply putting a constraint on the ocean model with SST observations; they translate to surface wind field and subsurface ocean memory. The SST data set used in this study is the reconstructed analysis of ref. 12 for the extended period of 1856–2003. Initialized with this monthly analysis, a forecast with lead times up to 24 months was made from each month of the 148-yr period. The same data set was also used to verify the model predictions.

Received 31 October 2003; accepted 26 February 2004; doi:10.1038/nature02439.

1. Fedorov, A. V., Harper, S. L., Philander, S. G., Winter, B. & Wittenberg, A. How predictable is El Niño? *Bull. Am. Meteorol. Soc.* **84,** 911–919 (2003).
2. Penland, C. & Sardeshmukh, P. D. The optimal growth of tropical sea surface temperature anomalies. *J. Clim.* **8,** 1999–2024 (1995).
3. Moore, A. M. & Kleeman, R. Stochastic forcing of ENSO by the intraseasonal oscillation. *J. Clim.* **12,** 1199–1220 (1999).
4. Thompson, C. J. & Battisti, D. S. A linear stochastic dynamical model of ENSO. Part I: Model development. *J. Clim.* **13,** 2818–2832 (2000).
5. Perigaud, C. M. & Cassou, C. Importance of oceanic decadal trends and westerly wind bursts for forecasting El Niño. *Geophys. Res. Lett.* **27,** 389–392 (2000).
6. McPhaden, M. J. & Yu, X. Equatorial waves and the 1997/98 El Niño. *Geophys. Res. Lett.* **26,** 2961–2964 (1999).
7. Boulanger, J. P. *et al.* Role of non-linear oceanic processes in the response to westerly wind events: New implications for the 1997 El Niño onset. *Geophys. Res. Lett.* **28,** 1603–1606 (2001).
8. Goswami, B. N. & Shukla, J. Predictability of a coupled ocean-atmosphere model. *J. Clim.* **4,** 3–22 (1991).
9. Chen, D., Zebiak, S. E., Busalacchi, A. J. & Cane, M. A. An improved procedure for El Niño forecasting: implications for predictability. *Science* **269,** 1699–1702 (1995).
10. Xue, Y., Cane, M. A. & Zebiak, S. E. Predictability of a coupled model of ENSO using singular vector analysis. Part I: Optimal growth in seasonal background and ENSO cycles. *Mon. Weath. Rev* **125,** 2043–2056 (1997).
11. Barnston, A. G., Glantz, M. H. & He, Y. X. Predictive skill of statistical and dynamical climate models in SST forecasts during the 1997/98 El Niño episode and the 1998 La Niña onset. *Bull. Am. Meteorol. Soc.* **80,** 217–243 (1999).
12. Kaplan, A. *et al.* Analysis of global sea surface temperature 1856–1991. *J. Geophys. Res.* **103,** 18567–18589 (1998).
13. Chang, P., Ji, L., Li, H. & Flugel, M. Chaotic dynamics versus stochastic processes in El Niño-Southern Oscillation in coupled ocean-atmosphere models. *Physica D* **98,** 301–320 (1996).
14. Latif, M. *et al.* A review of the predictability and prediction of ENSO. *J. Geophys. Res.* **103,** 14375–14393 (1998).
15. Zebiak, S. E. & Cane, M. A. A model El Niño-Southern Oscillation. *Mon. Weath. Rev.* **115,** 2262–2278 (1987).
16. Cane, M. A., Zebiak, S. E. & Dolan, S. C. Experimental forecasts of El Niño. *Nature* **321,** 827–832 (1986).
17. Jin, F. F., Neelin, J. D. & Ghil, M. El Niño on the devil's staircase — annual subharmonic steps to chaos. *Science* **264,** 70–72 (1994).
18. Tziperman, E., Stone, L., Cane, M. A. & Jarosh, H. El Niño chaos: overlapping of resonances between the seasonal cycle and the Pacific ocean-atmosphere oscillator. *Science* **264,** 72–74 (1994).
19. Zebiak, S. E. On the 30–60 day oscillation and the prediction of El Niño. *J. Clim.* **2,** 1381–1387 (1989).
20. Kirtman, B. P. & Schopf, P. S. Decadal variability in ENSO predictability and prediction. *J. Clim.* **11,** 2804–2822 (1998).
21. Balmaseda, M. A., Davey, M. K. & Anderson, D. L. T. Decadal and seasonal dependence of ENSO prediction skill. *J. Clim.* **8,** 2705–2715 (1995).
22. Davis, M. *Late Victorian Holocausts: El Niño Famines and the Making of the Third World* (Verso Books, New York, 2002).
23. Goddard, L. *et al.* Current approaches to climate prediction. *Int. J. Climatol.* **21,** 1111–1152 (2002).
24. Jin, F. F. An equatorial ocean recharge paradigm for ENSO. Part I: Conceptual model. *J. Atmos. Sci.* **54,** 811–829 (1997).
25. Meinen, C. S. & McPhaden, M. J. Observations of warm water volume changes in the equatorial Pacific and their relationship to El Niño and La Niña. *J. Clim.* **13,** 3551–3559 (2000).
26. McPhaden, M. J. Tropical Pacific Ocean heat content variations and ENSO persistent barriers. *Geophys. Res. Lett.* **30,** doi:10.1029/2003GL016872 (2003).
27. Kessler, W. S. EOF representation of the Madden-Julian Oscillation and its connection with ENSO. *J. Clim.* **14,** 3055–3061 (2001).
28. Smith, T. M. & Reynolds, R. W. Extended reconstruction of global sea surface temperatures based on COADS data (1854–1997). *J. Clim.* **16,** 1495–1510 (2003).
29. Rayner, N. A. *et al.* Globally complete analyses of sea surface temperature, sea ice and night marine air temperature, 1871–2000. *J. Geophys. Res.* **108,** doi:10.1029/2002JD002670 (2003).
30. Chen, D., Cane, M. A., Zebiak, S. E., Canizares, R. & Kaplan, A. Bias correction of an ocean-atmosphere coupled model. *Geophys. Res. Lett.* **27,** 2585–2588 (2000).

Acknowledgements This Letter was written during the sabbatical leave of D.C. at the Laboratory of Ocean Dynamic Processes and Satellite Oceanography, Second Institute of Oceanography, Hangzhou, China. This work was supported by the National Oceanic and Atmospheric Administration, and by the National Aeronautics and Space Administration.

Competing interests statement The authors declare that they have no competing financial interests.

Correspondence and requests for materials should be addressed to D.C. (dchen@ldeo@columbia.edu).

A lower limit for atmospheric carbon dioxide levels 3.2 billion years ago

Angela M. Hessler*, Donald R. Lowe, Robert L. Jones & Dennis K. Bird

Department of Geological and Environmental Sciences, Stanford University, Stanford, California 94305-2115, USA

* Present address: Department of Geology, Grand Valley State University, Allendale, Michigan 49401, USA

The quantification of greenhouse gases present in the Archaean atmosphere is critical for understanding the evolution of atmospheric oxygen, surface temperatures and the conditions for life on early Earth. For instance, it has been argued[1–4] that small changes in the balance between two potential greenhouse gases, carbon dioxide and methane, may have dictated the feedback cycle involving organic haze production and global cooling. Climate models have focused on carbon dioxide as the greenhouse gas responsible for maintaining above-freezing surface temperatures during a time of low solar luminosity[5,6]. However, the analysis of 2.75-billion-year (Gyr)-old[7] palaeosols—soil samples preserved in the geologic record—have recently provided an upper constraint on atmospheric carbon dioxide levels well below that required in most climate models to prevent the Earth's surface from freezing. This finding prompted many to look towards methane as an additional greenhouse gas to satisfy climate models[1,4,8,9]. Here we use model equilibrium reactions for weathering rinds on 3.2-Gyr-old river gravels to show that the presence of iron-rich carbonate relative to common clay minerals requires a minimum partial pressure of carbon dioxide several times higher than present-day values. Unless actual carbon dioxide levels were considerably greater than this, climate models[5,6,8] predict that additional greenhouse gases would still need to have a role in maintaining above-freezing surface temperatures.

Siliciclastic sedimentary rocks of the 3.2-Gyr (refs 10, 11) Moodies Group, Barberton Greenstone Belt (BGB), South Africa, include the oldest known non-marine deposits on Earth[11,12]. Basal clast-supported conglomerates of the Moodies Group have been interpreted to be alluvial fan and braided fluvial deposits on the basis of evidence for limited sediment reworking, periodic subaerial exposure, and unidirectional palaeocurrents[12]. The conglomerate is approximately 300 m thick and is dominated by pebbles and cobbles of chert, derived by erosion of deeper-level rocks of the Onverwacht Group, and porphyritic felsic volcanic and volcaniclastic rock, derived mainly from the immediately underlying Fig Tree Group. It also includes less-common (<7%) silicic plutonic rock, silicified ultramafic rock, greywacke, and quartzo-feldspathic sandstone.

Six pebbles showing distinctive dark outer layers or rinds were identified in drill core (73–113 m depth, well below the zone of modern weathering) of the basal Moodies conglomerate, at the Royal Sheba gold mine in the northern BGB (25° 43′ S, 31° 10′ E). These pebbles are aphanitic or microphyric with a fine-grained matrix of intergrown potassium feldspar, quartz and muscovite, with traces of carbonate (≪3%). In contrast, pebble rinds are characterized by an abundance of quartz and Fe(II)-rich carbonate (≫6%, $Fe_{0.53}Mg_{0.44}CO_3$), with lesser amounts of potassium feldspar and muscovite than observed in the pebble cores. The pebble rinds described here are marked by mineralogical changes to the outer 0.25–8 mm of the pebble, and should not be confused with caliche-like carbonate coatings. The Moodies Group conglomerate has experienced regional post-depositional alteration (primarily sericite and carbonate), and we cannot preclude the possibility that the carbonate in the rinds did not undergo ion exchange with diagenetic fluids. In fact, the high Mg^{2+} content at present observed in the rind carbonate is not probably primary, instead indicating partial Mg^{2+}–Fe^{2+} exchange with increasing burial temperatures[13]. However, the modal abundance of quartz and carbonate in the rinds compared with pebble interiors, and their textural fabric (see below), suggest a primary weathering origin for the rinds.

Textural and paragenetic relations demonstrate that the altered pebbles were rounded by river abrasion before the Fe(II)-rich carbonate rinds developed. Two of the pebbles show evidence of fracture during fluvial transport, and the alteration rinds are truncated against the fracture surfaces (Fig. 1). Petrographic and electron microprobe analyses show that the relative abundance of minerals near the fracture surfaces is like that of the pebble cores rather than the rinds[14]. If the rinds had formed during a pervasive post-depositional alteration, they would have developed along these fracture surfaces and around other clasts of similar composition. However, alteration rinds are rare on pebbles in this conglomerate, with most clasts of felsic volcanic rock (which make up 51% of the clast population) lacking visible rinds or geochemical evidence of surface alteration. Their rarity in the Moodies Group conglomerate is not surprising; weathering rinds seem to be inherently fragile features of stream-abraded pebbles. Sampling by the authors of modern stream cobbles from the Mojave Desert, the Klamath Mountains and the Sierra Nevada showed that only a small fraction of these cobbles contained the distinct Fe-oxide alteration expected in modern, weathered gravels[14].

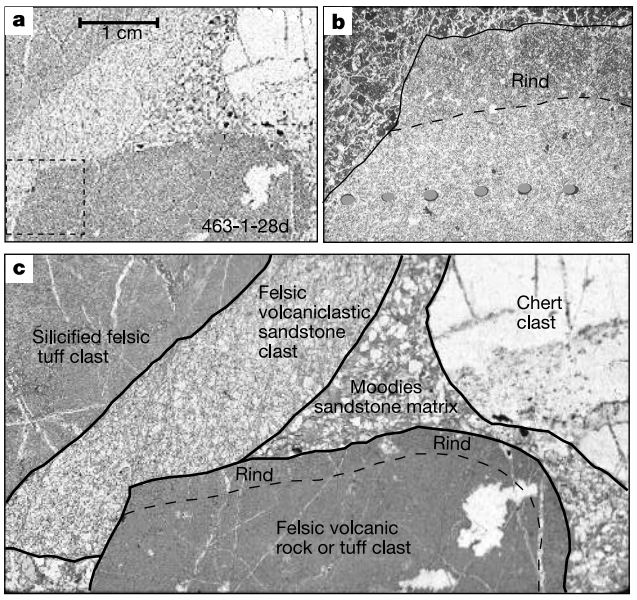

Figure 1 Microscope images of sample pebble 463-1-28d and its weathering rind. **a**, Scanned slide image of pebble 463-1-28d. A dark rind is visible around the outer 2 mm of this clast. **b**, Photomicrograph of the fractured edge of pebble 463-1-28d (see boxed area in **a**). The pebble edge is marked by the solid black line, and the interior extent of the rind is marked by a dotted line. The darkened rind is clearly truncated against the 'fresh' fracture surface. Grey dots were used as guides during microprobe analyses. **c**, A mapped version of **a**, to delineate clast types and matrix surrounding pebble 463-1-28d.